Liquid metal architectures for soft and wearable energy harvesting devices

IOP Publishing Multifunct. Mater. 4 (2021) 012001 https://doi.org/10.1088/2399-7532/abd4f0

Multifunctional Materials

TOPICAL REVIEW

Liquid metal architectures for soft and wearable energy harvesting devices

RECEIVED
19 September 2020

REVISED
16 November 2020

ACCEPTED FOR PUBLICATION
18 December 2020

PUBLISHED
12 January 2021

Mason Zadan[1], Cerwyn Chiew[2], Carmel Majidi[1,3] and Mohammad H Malakooti[2]

[1] Mechanical Engineering Department, Carnegie Mellon University, Pittsburgh, PA 15213, United States of America
[2] Mechanical Engineering Department, University of Washington, Seattle, WA 98195, United States of America
[3] Materials Science and Engineering, Carnegie Mellon University, Pittsburgh, PA 15213, United States of America

E-mail: cmajidi@andrew.cmu.edu **and** malakoot@uw.edu

Keywords: liquid metal, wearable electronics, energy harvesting, thermoelectric generators, triboelectric nanogenerators, dielectric elastomer generators, eutectic gallium indium

Abstract

Future advanced wearable energy harvesters need to have high power densities, functionality under large deformations, scalability, and robust resistance against mechanical damages (i.e. fatigue, delamination, and fracture). To achieve this, ultra-flexible, high dielectric, and thermally conductive materials along with deformable and robust electrodes are needed. Here, we review recent progress in synthesis and integration of liquid metal (LM) material architectures as the building blocks of emerging wearable energy harvesting devices. After a brief introduction to room temperature LM alloys, LM's various applications in a variety of soft and stretchable power harvesting devices including thermoelectric, triboelectric, dielectric elastomer, and piezoelectric generators are summarized. The unique opportunities and challenges introduced by LM material architectures in this field are also discussed.

1. Introduction

As wearable electronics become more readily available and used for more complex and diverse tasks, onboard human body generated power supplies have come alongside them to generate energy from biomechanical motion and heat generated from the body [1–7]. Each of these types of wearable energy harvesting devices can harness energy from the human body using different energy conversion mechanisms (figure 1(a)). For instance, wearable thermoelectric generators (TEGs) convert thermal energy from body heat to electrical energy through the Seebeck effect in which temperature differentials between the skin and the environment across positively and negatively doped semiconductors create a potential difference [6, 8, 9]. In contrast, wearable triboelectric nanogenerators (TENGs) and electromechanical energy harvesters—including dielectric elastomer generators (DEGs) and piezoelectric generators (PEGs)—generally convert biomechanical kinetic energy to electrical energy. These devices can scavenge energy from various modes of biomechanical motion on many points of the body such as the knee, hip, shoulder, elbow joint motion, and heel strike [10]. In particular, TENGs harness these biomechanical motions by electrostatic induction from the contact separation mechanism between materials with different intrinsic tendencies for gaining or losing electrons [11, 12]. DEGs generate energy from capacitive changes of charged electrodes sandwiching a dielectric elastomer sheet as it stretches and relaxes with biomechanical movement [13–16]. This human motion such as bending the knee or arm forces the charges to reconfigure on the elastomer as it is stretched, generating varying voltages. PEGs use active materials with high electromechanical coupling coefficients, which intrinsically converts mechanical deformations (i.e. pressure, vibration, body movement) into electrical signal or vice versa [17, 18]. They are widely used among commercial sensors and actuators [19–21] but increasingly utilized for wearable, flexible and wireless energy harvesting [22–26].

Compatibility between the device and the body has become an area of research for more conformable and efficient wearable systems. High elastic mismatch between skin and conventionally rigid electronics, poor breathability, and durability under large deformations are some of the common challenges. To address

Figure 1. Liquid metals in wearable energy harvesting devices: (A) image highlighting the applications and locations of LM based wearable electronics. Inset top left: liquid metal embedded elastomer based TEG. Reproduced with permission [27], copyright 2020, American Chemical Society. Inset bottom left: LM foam based shoe insert TENG. Reproduced with permission [28], copyright 2019, Elsevier Ltd. Inset top right: LM microfluidic and composite elastomer based wrist worn TEG. Reproduced with permission [29], copyright 2020, Elsevier Ltd. Inset bottom right: LMEE based joint worn TENG. Reproduced with permission [30], copyright 2020, WILEY-VCH Verlag GmbH & Co. KGaA. (B) Liquid metal embedded elastomer under deformation. Reproduced with permission [31], copyright 2017, National Academy of Sciences. (C) Liquid metal being poured (Indium Corp.). (D) Example of LM microfluidics. Reproduced with permission [32], copyright 2012, Institute of Electrical and Electronics Engineers.

these issues, soft and stretchable components are implemented, with special emphasis on the use of elastomers and textiles. While these soft components provide flexibility at some level, key rigid components are still required. These include stiff electrodes (e.g. copper for wiring) and thermal interfaces (e.g. ceramics for thermal management). As soft encapsulating components and rigid components interact with each other while trying to operate on the ever-changing morphologies of the human body, issues can occur. These issues include loss of contact between the device and body from the rigid components, short device lifetime due to the weak bonding and high stress concentration at the soft and rigid interface, and a lack of comfort for wearers. The more components of wearable energy harvesters that can be made soft and compliant to human movement, the more efficient, robust, and comfortable these devices will become.

To address the materials challenges, room temperature liquid metal (LM) alloys have stepped in to replace many traditionally rigid electronics components. For wearable applications, LM can be used to replace wiring [33–35], thermal interfaces [27, 31, 36], and dielectric materials [37]. This review highlights recent progress with the incorporation of LM into wearable energy harvesting and presents a discussion on differences in performance between LM based and non LM based wearable energy harvesters.

2. Overview of LM architectures

Liquid metallic alloys of gallium (Ga) such as EGaIn are liquid at room temperature, have low viscosities, high thermal conductivities (20–30 W m^{-1} K^{-1}) [38–40], high electrical conductivities (1–4 $\times$ 10^6 S m^{-1}) [41] and low toxicities [42, 43]. To harness these properties in wearable electronics, LMs can be packaged as microfluidics [44–54], and LM embedded elastomer (LMEE) composites [31, 55–62] (figures 1(b)–(d)). Design constraints for wearable energy harvesters are conformability with a user's skin, biocompatibility, structural integrity, and stable functionality (i.e. thermal and electrical properties) [63–66]. LM microfluidics and LMEE are two current LM material architectures enabling structural and functional properties that can satisfy these desired attributes.

LM microfluidics are LM traces embedded in elastomers such as polydimethylsiloxane (PDMS) that can act as electrodes and wiring in wearable electronics and sensors [67, 68]. This material architecture can retain its electrical conductivity when bent [69] or even stretched above 700% strain [70], and with a dynamic viscosity of only 2.2 times that of water [71], this makes them ideal electrodes for applications in stretchable electronics as they replace traditional stiff metal electrodes [39, 44]. They can be fabricated by LM injection,

stencil lithography, vacuum filling, and selective surface wetting into precured polymer molds before being covered by another layer of uncured polymer for final curing [33, 72–75]. Stencil lithography is one of the most common fabrication techniques [73, 75, 76]. A stencil mask is placed over the device and LM is sputtered onto the surface. The mask is removed leaving deposited LM at the proper locations. This is common for depositing LM in a controlled manner with traces as small as 200 μm wide and as small as 100 μm apart [75]. More recent work has been able to create LM traces as narrow as 30 μm by prestretching PDMS before patterning by stencil lithography [77]. For thin sheet electronic devices in particular, LM nanoparticle (LM NP) thin films are another fabrication approach for deformable electronics [78, 79]. This approach uses insulating Ga_2O_3 encased EGaIn NP that, once mechanically or laser sintered [80], create conductive traces. Such thin-film traces of EGaIn can be as thin as 1 μm [78].

LMEEs are a class of soft multifunctional composites prepared in the form of an emulsion of micro or nano sized droplets of LM dispersed in an elastomer matrix material [55, 81, 82]. These composite materials retain the mechanical properties of elastomers while having an excellent thermal conductivity [57, 83] of 1.6 W m^{-1} K^{-1} for a 1:1 LM to elastomer volume ratio [31], high dielectric properties [37, 56, 61], and an ultra-high fracture toughness [84]. In addition, LMEEs' strain limit can reach as high or higher than most elastomers [31] with one studying identifying a strain limit of 680% [58]. LMEEs can be fabricated as electrically conductive [59, 60] or insulating depending on their LM fill percentage and interface properties. LMEEs that are fabricated as electrically insulating can be made electrically conductive when activated with mechanical pressure as the non-percolating LM inclusions are sintered together rupturing their native oxide skins and bridging the adjacent inclusions by deployed liquid phase core. This creates percolating and controllable pathways of LM within the LMEE, thus creating electrically conductive channels acting as electrodes or LM wiring [62]. These percolating networks can replace LM microfluidics for wiring and are self-healing with damage to a pathway causing the pathway to reconfigure around the damage, often leading to a drop in resistance [85]. With an electrical conductivity of $\sigma = 1.37 \times 10^5$ S m^{-1} these pathways are sufficiently conductive to replace copper [62]. In addition to mechanical sintering, the solid–liquid phase transition of the embedded LM droplets can also be utilized for inducing electrical conductivity [58, 86]. Although this activation process is reversible, it does not apply to LM nanocomposites due to the suppressed melting and freezing temperature of LM nanodroplets [81]. LMEE is stable under extreme environmental conditions if the size of LM inclusions is sufficiently small and the elastomer matrix is stable under these conditions. In a recent study, it was shown that with the selection of Sylgard 184 as the matrix and encapsulation of EGaIn micro-/nanodroplets (<3 microns in diameter), the LMEE composite can stand to temperatures as low as −80 °C, suitable for flexible thermoelectric wearables in extreme weather conditions [36]. Although, the same study showed that the supercooling feature of LM nanodroplets is independent of the polymer coating or substrate along with the synthesis method used for fabricating these materials, it is crucial to ensure the polymer matrix is also stable at these conditions. Another advantage of polymer composites with nanoscale LM inclusions is eliminating the reactivity and corrosive behavior of Ga-based LMs. It has shown that EGaIn nanodroplets (100–800 nm in diameter) exhibit high stability and negligible corrosion effect even in direct contact with metals such as aluminum [87]. This is mainly due to the protective oxide layer on the LM nanodroplets which prevents the Ga ions in the liquid core to react with other metals.

These multifunctional properties of LM elastomer composites along with their feasible and scalable fabrication process can be advantageous for applications in wearable energy harvesters. In particular, such materials can serve the role of highly compliant thermal and electrical interfaces, interconnects or both. In the past, researchers have synthesized soft polymer composite with stiff conductive fillers such as silver nanowires/flakes [88–90], gold NPs [91], carbon nanotubes [92, 93], and gold nanosheets [94] to form percolative networks of electrically conductive pathways. These rigid fillers can lower the mechanical compliance of the host elastomers and introduce defects due to nonuniform filler dispersion. This has made soft-LM composites a preferred material of choice for wearable technologies and soft robotics. Since wearable energy harvesters can be subjected to large deformations from users' stimulus (i.e. arm bending, leg bend), LMEE composites are able to appropriately deal with these changing morphologies while fulfilling their role in their respective systems. The following sections will cover the implementation of such LM material architectures to solve various problems in wearable energy harvesters.

3. Thermoelectric generators

3.1. Background and physics of TEGs

Thermoelectric energy conversion in which heat is directly converted to electricity has been considered a power source for wearable electronics [6, 8, 95]. Wearable TEGs recover the wasted heat energy from the human body by using the Seebeck effect in which temperature gradients (∇T) between the skin (heat source)

and ambient air (heat sink) applied across parallel p (electron donating) and n (electron receiving) type semiconductors induce current flow [3]. The effectiveness of these semiconductors is captured by the semiconductors figure of merit (ZT), which is described as

$$\mathrm{ZT} = \frac{\alpha^2 \sigma}{\lambda} T, \tag{1}$$

where α is the Seebeck coefficient, σ is the electrical conductivity, λ is the thermal conductivity, and T is the temperature [96]. The TEG output power (P_{TEG}) depends on semiconductor Seebeck coefficient α, local thermal gradient (∇T) and the electrical conductivity (σ) [96]. Researchers have used LM microfluidics as flexible electrical electrodes [97] and LMEE as thermal interfacing between skin and the TEG [27]. These approaches ensure that TEGs have high internal electrical conductivity (σ) and large thermal gradient (∇T) across the TEG, which is achieved by maintaining skin to TEG contact even under large deformations. Optimizing these factors maximizes the power output of the TEG where $P_{\mathrm{TEG}} = (\alpha \nabla T)^2 \sigma$.

3.2. Fabrication methods of previous non-LM wearable TEGs

One of the major challenges is to provide sufficient mechanical compliance to suit such applications. Flexible thermoelectric modules have been developed through different fabrication techniques including the use of solution processable organic semiconductors [98, 99], fiber-based devices and textiles [100–105], printable nanosheet and thin film based devices [106–108], a screen printed and polymer hybrid device [109], and encapsulation of rigid inorganic semiconductors in soft elastomers [4, 110]. Different material architectures across multiple length scales have been used for fabrication of flexible TEGs. For instance, pellet semiconductors have incorporated soft packaging materials such as PDMS in an effort to replace traditional materials such as copper and ceramics to better harvest energy. This is due to an increased contact area with skin and efficient thermal transport at the material interfaces, enabling interfacing with other wearable devices while maintain high thermal absorption from the skin [111–114]. Moreover, these devices can be utilized to power other wearable electronics like an ECG device [4, 110]. Other wearable TEGs have incorporated nanosheets of printable semiconductors on polyimide and flex PCB to fix rigidity and thickness issues raised by pellet based semiconductors for wearable applications [106, 115–118]. While these nanostructured TEGs are extremely thin and bendable, their voltage and power generation is quite low with 16.9 nW and 4.8 mV, respectively, at a temperature gradient of 47.2 °C [106]. Moreover, some implementations require silver wires and silver paste to wire the semiconductors together [115].

3.3. LM screen printing for wearable TEGs

More recent work has begun to incorporate LM into nanowire-based printed semiconductor TEGs in order to reduce the contact resistance between different components. Using LM screen printed interconnects, this device recorded the highest power values at the time of publication for this class of thin-film device (table 1) [119]. Using low-temperature solution-phase synthesis methods [120], bismuth telluride (Bi_2Te_3) and bismuth antimony telluride semiconductors were integrated using a nanowire-based printable ink. Once formulated, the semiconductor ink was inkjet printed onto a polyimide base layer. Using stencil lithography, EGaIn was selectively deposited with a nitrogen assisted spray coating procedure to create flexible interconnects between the p and n type semiconductors. The device was then sealed with a silicone elastomer. The authors reported that when compared to using silver paste for the interconnects, EGaIn interconnects increased flexibility of the device [119]. The device tested had five thermoelectric modules and recorded a maximum power output of 127 nW at $\Delta T = 32.5$ °C. At temperatures consistent with the ambient environment and human body, the TEG generated 14.1 nW and 10.5 mV at $\Delta T = 7$ °C. While these devices are extremely thin and can deform well to the human body, even with LM's incorporation, their low power limits their applicability for wearable devices.

3.4. LM microfluidics for TEGs

Comparatively, pellet-based semiconductors (which are used in commercially available TEGs) embedded in elastomer composites, pose a solution to these low energy harvesting issues. Pellet based TEGs represent a more traditional design, with semiconductor pellets/cubes connected in series to create a Seebeck effect. The electrical and mechanical performance of pellet based TEGs has also been improved with the development of LM material architectures. For pellet based TEGs, LM was first proposed as an approach to mitigate thermal stress between semiconductors and their connectors [122]. The first device to begin to realize this potential was published over 10 years later in 2017 [97]. It was based around a 16-semiconductor array of Bi_2Te_3 pellet semiconductors that were suspended in an Ecoflex™ elastomer matrix (figure 2(a)). This device was fabricated in layers with stencil lithography again being used to create LM interconnects [97]. The semiconductors, which were prewetted with LM, were then placed in series with Ecoflex filling in the open

Table 1. Comparison of LM based TEGs.

LM material architecture implementation	# of semiconductors	Power/ power density	Voltage	Bending and strain cycles	Device internal resistance	Ref.
Interconnects	10	14.1 nW @ $\Delta T = 7$ °C 127 nW @ $\Delta T = 32.5$ °C	10.5 mV 46 mV	50 bending cycle 0% $\Delta\Omega$	3.9 kΩ	[119]
Interconnects	16	19.8 μW cm^{-2} @ $\Delta T = 20$ °C	∼22 mV	1000 20% stretching cycles −10% $\Delta\Omega$	∼1.75 Ω	[97]
Interconnects	64	46.28 μW @ $\Delta T = 1.1$ °C	8.22 mV	1000 bending cycles 0% $\Delta\Omega$	1.26 Ω	[121]
Interconnects	64	Device on wrist with 1.2 m s^{-1} fan ∼45 μW cm^{-2}	∼45 mV	250 bending cycles 0 ± 0.5% $\Delta\Omega$	6.5 ± 0.5 Ω	[29]
LMEE for interconnects and thermal regulation	100	1.68 mW (86.6 μW cm^{-2}) @ $\Delta T = 60$ °C	59.96 mV @ $\Delta T = 10$ °C	1000 30% stretching cycles 21% $\Delta\Omega$ 50% strain ∼12% $\Delta\Omega$	∼13.5 Ω	[27]

spaces. The same process was completed on the top side with Ga deposited again as interconnects and sealed with another layer of Ecoflex. The fabricated devices dimensions were 1.5 × 2.0 cm. At $\Delta T = 20$ °C with resistance load matching, the device's recorded power density was 19.8 μW cm^{-2} with one thermoelectric module generating ∼3 mV. The major improvement of this system to previous work is that LM was used as the interconnect material instead of copper or, in some cases, flex PCB [123]. The use of LM allowed for the device to stretch while guaranteeing solid semiconductor to interconnect contacts. Compared to previous semiconductor pellet based TEGs, this device does not fail mechanically or electrically under linear cyclical loading. After 1000 cycles of 20% strain the internal resistance of the device actually decreased by 10% as the loading improved interconnect semiconductor contact [97]. Rigid electrodes often used for interconnects have been identified as a major limiting factor in stretchable electronics in a past review [64].

This fabrication approach and architecture continues to be widely adopted, with another paper in 2017 implementing 32 Bi_2Te_3 thermoelectric modules suspended in a PDMS matrix with LM interconnects [121]. The semiconductors were pre-wet with EGaIn, followed by EGaIn traces deposited onto the surface connecting the legs together. The completed device had a TEG area of 4 cm^2 (figure 2(b)). To better emulate real world applications, this TEG was tested on skin with the temperature differential calculated in different air velocity environments and ambient temperatures. The performance of this device was limited with the maximum voltage and power being 0.69 mV and 0.33 μW (0.0825 μW cm^{-2}) respectively at $\Delta T = 0.09$ °C for an air velocity of ∼0.9 m s^{-1}. At $\Delta T = 0.4$ °C with no air velocity the device recorded results of 1.47 mV and 1.48 μW (0.37 μW cm^{-2}). The highest recorded values were 8.22 mV and 46.28 μW at $\Delta T = 1.1$ °C. The lack of proper thermal and insulating materials leads to a degradation in the thermal gradient over time. This leads to a loss of power and voltage when applied to the body for long periods of time when applied to the body. One test saw the voltage drop by 17% and power by 30% after ∼40 min on skin. This device was cyclically bent in order to test its ability to move and deform on the human body. Over 1000 cycles with a 5 mm radius bend the TEG showed no degradation of resistance and even self-healed during three separate occasions during loading highlighting the robustness of this material architecture for wearable energy harvesting compared to non-LM work. A later study used a similar approach but implemented flex PCB boards instead of LM on the underside of the device to act as interconnects and to help ensure good contact with the body [124]. PDMS was again used to hold the device together with LM deposited in grooves on a sealed top layer as interconnects. Although the flex PCB has a low thickness and can conform to the skin, it increases the complexity of the device requiring extensive amounts of soldering and limiting the device from stretching. This design choice of both LM and flex PCB interconnects also led to visible structural integrity issues.

3.5. LMEE for wearable TEGs

These previous devices address issues related to flexibility and electrical connectivity that stem from poor contacts and an inability of the rigid interconnects to deform under tensile strain. However, they still lack proper thermal management and there still remains to be significant room for improvements in energy harvesting performance. One issue is that PDMS elastomer has a low thermal conductivity of 0.18 W m^{-1} K^{-1}, making it an insulator [125]. It is not a proper material for holding temperature gradients

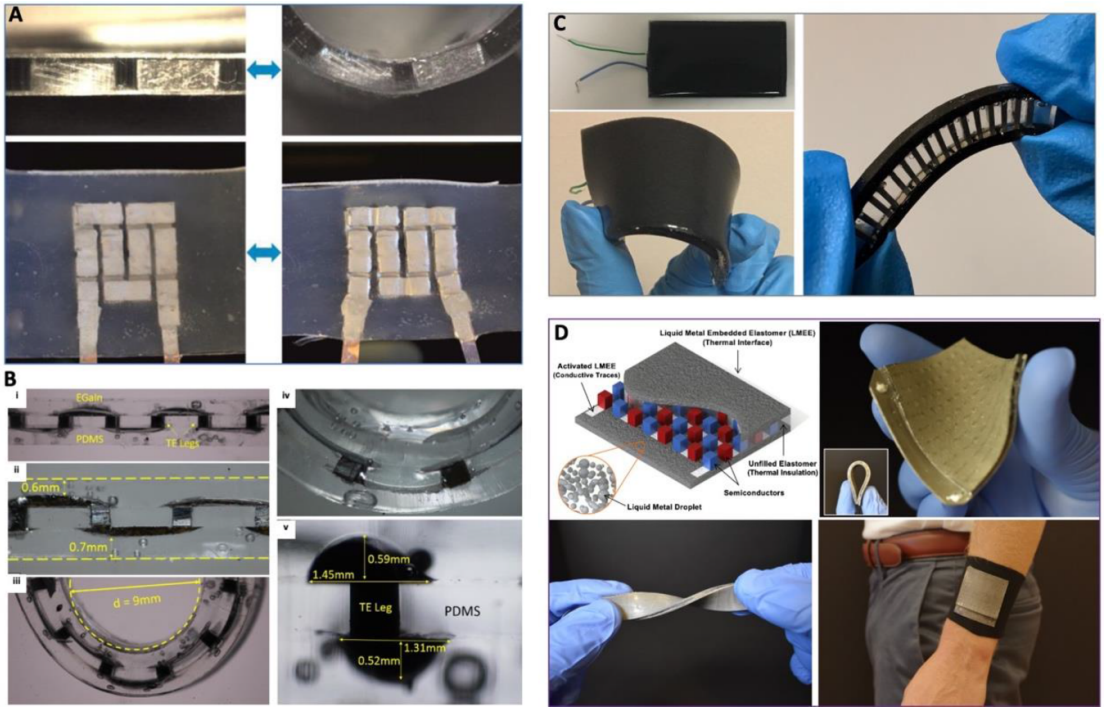

Figure 2. Liquid metals in thermoelectric generators: (A) unstrained vs strained image of the first LM based elastomer pellet TEG with images highlighting the movement of the semiconductors during bending. Reproduced with permission [97], copyright 2017, American Chemical Society. (B) Images highlighting the incorporation of LM as interconnects between pellet semiconductors in an elastomer matrix along with highlighting bending abilities. Reproduced with permission [121], copyright 2017, Elsevier Ltd. (C) TEG with LM based high thermal conductivity surface layer and LM interconnects highlighting deformation. Reproduced with permission [29], copyright 2020, Elsevier Ltd. (D) Top left: schematic of the first soft and stretchable TEG enabled with multifunctional LMEE composite, top right: a 100-semiconductor (Inset: 18-semiconductor) TEG under deformation, bottom left: twisting an intact 16-semiconductor TEG after 1000 cycles of 30% strain, bottom right: the TEG device on the user's wrist. Reproduced with permission [27], copyright 2020, American Chemical Society.

between the sides of a TEG, which is key for proper power generation. PDMS is not ideal for two reasons. As an insulator it cannot absorb heat from the body well nor release the heat on the cold side of a TEG. Separately, the use of a single layer of elastomer allows for heat to transfer from one side to the other decaying the temperature difference between the two sides of the pellet semiconductors. To fix this problem LM elastomer composites were introduced as thermal interfaces into TEGs.

LMEE has already been introduced as a thermal absorber and heat sink for TEGs, enabling fabrication of a cold-resistant self-powered 'electronic sleeve' for monitoring an individual's heart rate at low temperatures (0 °C or lower) [36]. Compared to unfilled PDMS, LMEE thermal interfaces have shown significantly higher efficiency when used with conventional rigid TEGs. Since the EGaIn–PDMS composites are extremely compliant, they provide a better conformal contact over a large area, which results in a comparable performance when compared to unpackaged rigid thermoelectric modules. These thermally conductive elastomers have become a popular choice for flexible thermoelectric energy harvesters. A recent study has incorporated EGaIn and graphite nanoplatelets into an elastomer matrix to increase thermal conductivity at the interfaces (figure 2(c)). Similar to the previous study, the high thermal conductivity of the elastomeric nanocomposite greatly outperformed unfilled PDMS. LM traces were again used for the interconnects between the semiconductors in this study [29].

The most recent work in this field builds on these previous approaches and uses LMEE to implement LM as both a thermal material and, through mechanical activation of its surface, as electrical interconnects for the semiconductors (figure 2(d)) [27]. This solves the problems of thermal management, rigid interconnects, and complex design processes requiring LM to be deposited separately onto the surface and then sealed into the device. The device is fabricated in three layers with LMEE on the top and bottom and a film of PDMS in between that contains the Bi_2Te_3 semiconductors. The undersides of the LMEE was patterned creating traces to act as the interconnects for the thermoelectric modules. The PDMS center sheet was cured and then laser cut to hold 100 rigid semiconductors (i.e. 50 pairs of n-type and p-type thermoelectric modules). To bond these pieces together, oxygen plasma treatment was used [126, 127]. The components were aligned and then cured. This work generates excellent power and voltage with its new thermal management advantages exceeding all previous LM TEGs. At $\Delta T = 10$ °C, 60 mV was recorded with differences of 80 °C generating

more than 400 mV. Resistance matching the internal and external loads at $\Delta T = 60$ °C gave a max power of 1.68 mW and power density of 86.6 μW cm^{-2}. The internal resistance of ~13.5 Ω was measured at room temperature. Other unique features of these wearable TEGs are high stretchability and durability due to the elimination of rigid interconnects. During cyclical and tensile loading, the device did not electrically or mechanically fail indicating the excellent structural integrity and functional stability of the device. Using an 18-semiconductor version of the TEG as a tensile specimen for electromechanical testing, failure occurred between 50% and 70% strain with the internal resistance increase below 20%. The tensile specimen was also cyclically loaded at a 30% strain for 1000 cycles with no mechanical or electrical failure with a 21% increase in resistance. These excellent strain results are attributed to the simple design process of incorporating LMEE as a deformable thermal and electrical interface.

While these devices have been improving in thermoelectric performance over time, they still lack the performance of traditional rigid commercial TEGs. For example, by comparing the performance of a 40 × 40 mm and 256 semiconductor commercial TEG (TEG2-126LDT Scavenger TEG module) to the TEGs in table 1, a significant difference in performance is found. At $\Delta T = 15$ °C, $V_{oc} = \sim$800 mV and the matched load output power is ~30 mW for this commercial device, highlighting the improvements that will need to be made for deformable TEGs to eventually enter the commercial space.

4. Triboelectric nanogenerators

4.1. Physics of TENGs

TENGs have attracted considerable attention as a low frequency energy harvester for wearable technologies. TENGs excel in their ability to convert ambient mechanical energy into electrical energy while being lightweight, having a simplistic design, and allowing the use of inexpensive materials for fabrication. Mechanical motion can drive the contact separation modes (i.e. vertical, sliding or both) of a pair of distinct dielectric layers in contact, each with inherently different tendencies to release or receive electrons [11, 128]. This tendency is quantified by their rank within the triboelectric series. This contact separation mode causes coupling of triboelectric and electrostatic induction to generate current and power.

The triboelectric effect is comparable to the Van der Graaf generator [129], which consists of a metal dome that becomes highly positively charged through internal friction of a rotating rubber belt. This charging occurs through continuous electron removal by a dielectric material before eventually being neutralized by abrupt electron donations from the ground. This can be observed as a sudden corona spark discharge. The positive charging of the metal dome and the charge leakage phenomena are analogous to a user's skin rubbing or pressing onto TENG's surface followed by the induced current, respectively.

4.2. Review of early devices

Natural biomechanical motion such as arm flexing, gaiting, hip motions, and tactile actions can deform wearable TENG devices which in return generate large output electrical power. The first TENG was made of paired unbonded polymer films sandwiched by gold films with a power density of 10.4 mW cm^{-3} [130]. Bending of the film laminates causes frictional agitation between the polymer film, inducing electrostatic effects and current flows. Since then, TENG designs have been developed by harnessing a wider range of mechanical motion such as press and release and rotational motion with improved charge trapping abilities. This improvement was fabricated by micro-texturing the contact surface to increase surface area for more electron exchanges to occur [131, 132]. Despite its decent power density, the Young's modulus mismatch of gold electrodes and polymer laminates can reduce the range of TENG deformation. This degrades its maximum power efficiency potential, restricts bending deformability, and creates lower durability or fatigue life. These drawbacks have prompted researchers to pursue more advanced electrode materials for wearable TENG that have enhanced dual mechanical durability when strained and with excellent charge-trapping properties.

4.3. LM microfluidics for TENGs

One of the earliest choices of electrodes to solve this problem is to utilize liquids or liquid-infused materials such as microfluidic architectures with ionic solutions [133, 134] or ionic hydrogels [135, 136]. Alternatively, LMs have garnered recent traction as a solution to these issues because of its better mechanical and chemical stability compared to ionic liquids. This is likely due to the native oxide skin of Ga-based LM alloys like EGaIn [52, 54, 78, 137, 138]. TENGs based on a single LM microfluidic electrode are generally fabricated by transferring LM into micro patterned channels of partially cured elastomer before being sealed with another uncured layer prior to additional complete curing. This embedded electrode is capable of stretching up to 300% strain while remaining electrically conductive since conductive bulk LM will continuously fill the elongated fluidic channel during deformation [52]. These electrode features are highly beneficial for

Table 2. Performance comparison for different LM architecture in TENG devices.

LM architecture	Power/power density	Max V_{OC}	Stretchability/strain cycles/resistance change	Device internal resistance	Ref.
Electrode (NP film)	3.23 mW	268 V	260%; 2000 cycles ∼3% $\Delta\Omega$	20 MΩ	[139]
Dielectric interface (LMEE)	13.95 mW m^{-2}	60 V	100% strain @1500 cycles ∼79% $\Delta\Omega$	100 MΩ	[138]
Dielectric interface (LMEE)	13 μW cm^{-2}	200 V (Jogging on insole)	100% strain @88 nC per cycle; other information N/A	Not Reported	[28]
Dielectric interface and electric electrode (Functionally graded LMEE)	1 mW cm^{-2} (area) 3.2 mW g^{-1} (Weight)	604 V (Max)	500% limit; 10 000 cycles reliability, Negligible open circuit voltage change	1.1–1.7 GΩ depends on volume fraction of LM	[30]

wearable TENG because it ensures maximum extraction of charge flows/current (i.e. unchanged resistance) even during large deformation (i.e. knee or arm flexion movements) allowing possible fabrication of a functional 3D TENG. This type of electrodes allows control over the geometry of the electrical pathways in TENGs as a design parameter. For instance, LM interdigitated [49] and spiral [50] electrodes have been used to harvest energy in either vertical separation or lateral sliding modes (hand patting and rubbing). Both configurations allow the TENGs to function as stretchable self-powered capacitive or proximity sensors, but the latter design can also function as a force sensor. However, such LM microfluidic based electrodes can leak by impulsive or dynamic mechanical damage to the TENG that may rupture the encapsulating elastomer layer. This can be mitigated by using a mixture of shear stiffening gel (SSG) and an elastomer as the encapsulating matrix material for the LM microfluidics [51]. A SSG is viscous at rest (or at low frequency deformation) and becomes rigid upon impact (high frequency deformation) due to having a larger storage modulus (i.e. stiff) at high frequencies. Introduction of SSG into elastomers protects LM content of electrode when stretchable TENG is inflicted by sudden extreme mechanical impact or damage.

In the pursuit of lightweight and thinner wearable TENGs, electrodes are required to be ultrathin while not sacrificing conductive and deformable performance, prompting researchers to use LM NP thin films as an alternative to microfluidic type electrodes (table 2) [139]. This thin-film device consists of clusters LM NPs (<1 μm diameter) that have large effective surface areas, each with electrically insulating oxide shells (∼3 nm thick). The sintering process coalesces the LM NPs to form wide electrically conductive pathways during stretchable TENG fabrication. Thinner electrodes of TENGs can enhance its sensitivity to tactile stimuli but will have limited stretchability up to 100% before conductance drastically drops (figure 3(a)) [139]. Since, LM NPs electrode will have smaller conductive LM content than microfluidics, upon large applied strain (1.0–2.5 stretch ratio), there will be increased resistance up to 2× because of the increased detachment of coalesced networks of conductive LM NPs (i.e. reduced percolation effect).

4.4. LMEE for TENGs

It is mentioned that LM elastomer composites possess dual dielectric and human skin-like compliant properties that have encouraged researchers to explore LM polymer composites for improving TENG performance as both an electrode and charge trapping material. Based on recent works, LMEE has been used as either the triboelectric dielectric component with high dielectric properties (figure 3(b)) [138] or as both electrode and triboelectric component (figure 3(c)) [30]. Recently, it has been shown that LMEE can increase the surface charge density of triboelectric components and reduce surface leakage charge at contact layers by using LMEE with higher dielectric constants [141]. The high dielectric constant of LMEE (ε_{LMEE}) allows for increased surface charge density (σ). Using the expression for TENG output voltage (V) [142]:

$$V = \frac{\sigma x(t)}{\varepsilon_0} - \frac{Q}{S\varepsilon_0}\left(x(t) + \frac{d}{\varepsilon_{\mathrm{LMEE}}}\right) \tag{2}$$

where ε_o, $x(t)$, Q, S, and d are the electrical permittivity in vacuum, time-dependent gap difference of the electrodes, number of transferred charges between the electrodes, contact area, and thickness of the dielectric material, respectively. High dielectric constant LMEE composites will increase the values of σ and $\varepsilon_{\mathrm{LMEE}}$, thereby maximizing output voltage as well as minimizing surface leakage effects (2nd term in equation (2)).

Another TENG design incorporates dual electrode and triboelectric layers with a porous composite of LMEE, which is termed a liquid-metal-elastomer foam (figure 3(d)) [28]. To increase surface charge density within this composite and induce electrostatic current during mechanical deformation, the surface of the

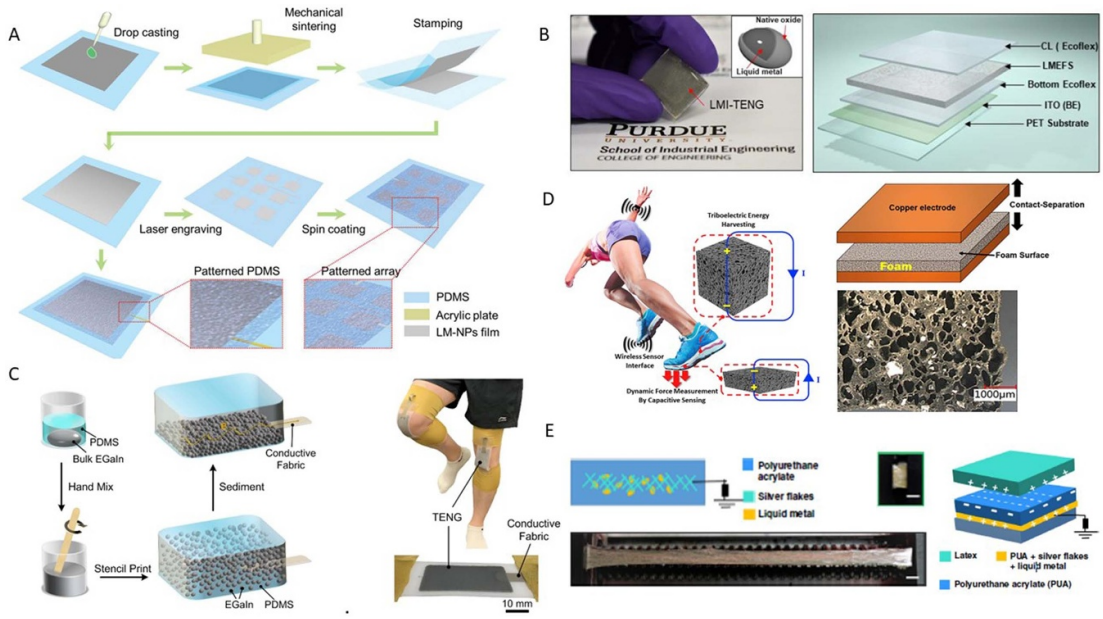

Figure 3. Liquid metals in soft and wearable triboelectric generators: (A) LM based E-skin triboelectric generator with touch sensing capabilities. Reproduced with permission [139], copyright 2020, WILEY-VCH Verlag GmbH & Co. KGaA. (B) Liquid metal elastomer composite as dielectric tribomaterial. Reproduced with permission [138], copyright 2019, The Royal Society of Chemistry. (C) Functionally graded liquid metal elastomers as tribomaterial and electrodes in a TENG with large stretchability. Reproduced with Permission [30], copyright 2020, WILEY-VCH Verlag GmbH & Co. KGaA. (D) Liquid metal elastomer foam composite for triboelectric generators. Reproduced with permission [28], copyright 2019, Elsevier Ltd. (E) LM acts as an electrical anchor for silver flakes in a PUA matrix for a self-healing TENG with 2500% hyperstretchability. Reproduced with Permission [140], copyright 2019, Springer Nature Limited.

interior inclusions of this foam become contact layers with each inclusion acting as miniature triboelectric generator as the foam compresses and releases. Most of these studies integrating compliant LMEE as triboelectric layers for TENGs still use stiff metal electrodes (gold and copper), which negates the overall deformability of the TENG. As discussed in the TEG section, LM electrodes help solve the rigidity issues that copper and rigid electrodes have in soft devices. More recent work has solved this problem by incorporating LMEE as a functional electrode and triboelectric component of TENG [30]. In this study, the LM droplets are non-uniformly distributed through the thickness of LMEE in order to create a functionally graded LMEE composite for wearable TENGs (figure 3(c)). This is achieved by suspension of large EGaIn inclusions in uncured elastomer, which settle to the bottom prior to the curing process. Two regions, an elastomer-rich and an LM-rich region, form in this material. This is referred to as 'sedimented liquid metal elastomer'. The elastomer-rich side serves as the triboelectric layer, while the LM-rich side performs as an electrode. Unlike sandwich structured TENGs, this TENG configuration creates a gradual increment of Young's modulus over the thickness of LMEE, reducing the delamination effect from bending, while increasing fatigue life. The result is a LMEE based stretchable TENG with high stretchability (>500%), skin-like softness (<60 kPa), and high electrical/mechanical durability (>10 000 cycles). With these mechanical improvements, this technology has been integrated into highly stretchable fabrics for exercise clothing, while exhibiting a peak power area density of 1 mW cm^{-2} [30].

4.5. Other LM approaches for TENGs

A recent study uses LMs welding of low dielectric polymer fibers (i.e. polyacrylonitrile) in elastomer composites as the TENG active layer and requires smaller amounts of expensive LM (<1.5 weight %) during fabrication. This device achieves a max power area density of 4 W m^{-2} even after 800 contact cycles on the device. Similarly, this modified LM architecture, resembling LMEE, improves the charge-trapping capability of the triboelectric layer [143]. Another study uses a low weight percentage of LM fillers with rigid silver flakes embedded in a self-healing polymer (polyurethane acrylate (PUA)). This material architecture creates a self-healing stretchable TENG as shown in (figure 3(e)) [140]. This self-healing TENG can be stretched to an impressive 2500% strain and regain its energy harvesting performance even after extreme mechanical damage despite its electrodes being made of rigid conductive fillers (i.e. silver flakes) [140]. In this study, ruptured LM NPs act as percolative nodes or electrical anchors for silver flakes when hyper-stretched (>2000%) to reduce resistance increment. Upon mechanical damage, this electrode composite can be heated

for self-healing of the PUA matrix, regaining its stress–strain behavior close to its pre-damaged state. At the optimum load resistance of 1 MΩ, the output power density was 40 μW cm^{-2}.

5. Electromechanical energy harvesters

5.1. Dielectric elastomer generators

5.1.1. Physics of DEGs

While wearable TENGs incorporate dielectric materials to generate electricity from friction and contact forces between dielectric elastomers, a new class dielectric elastomer generators (DEGs) has been developed that generates energy purely from the electromechanical coupling of dielectric elastomers. Compared to other actuation based energy generators such as piezoelectric, variable capacitor, and electromagnetic generators, dielectric elastomers have advantages due to their low density, large actuation strain and speed, and high specific energy density [144–146]. DEGs convert mechanical work to electrical energy. This relationship is given as electromechanical coupling and describes the dielectric materials' ability to convert mechanical to electric energy. This helps to describe the effectiveness of soft elastomers for DEGs [147]. In order for a DEG to operate, the elastomer is first strained and then a charge is applied to the strained elastomer. Actuation begins with the elastomer being relaxed to zero strain. The changing thickness and surface area of the elastomer along with the constant charge on the dielectric material creates varying potential differences as charge densities and capacitance vary during actuation. The generated voltage is then sent to a capacitor to store the energy and the process repeats.

5.1.2. Early elastomer DEGs

Research has focused on acrylic and silicone-based elastomers as dielectrics on account of their breakdown strength, deformability, and low mechanical and electrical loss [13, 14]. An early acrylic DEG was published in 2001 based on heel strike actuation with a follow up study published in 2012 [13, 145]. This device was placed in the heel of the shoe and generated energy through mechanical pressure. The device was made with 20 elastomer layers in a diaphragm arrangement which generated 0.8 J per step and about 1 W of power. The device was able to power night vision goggles and had a power density of 0.3 J g^{-1} [13]. More recent research has focused on cone-shaped actuator designs that use a single elastomer layer and are simple to fabricate. One example is a polyacrylate elastomer (3M VHB4905) DEG with a thickness of 500 μm that recorded an energy density of 130 mJ g^{-1} with an electromechanical coupling conversion efficiency of 25% [148].

5.1.3. LMEE based DEGs and their advantages

While unfilled elastomers have been popular for DEGs, researchers have also explored the use of polymer composites with enhanced electrical permittivity. These are composed of elastomer that is embedded with a suspension of filler particles. Such particles can be dielectric or conductive and have included non-ferroelectric fillers such as titanium dioxide, ferroelectric NPs such as barium titanate ($BaTiO_3$), Ag flakes, Ni and Ag NPs, and carbon nanotubes [149–152]. While these composites have increased dielectric properties, the rigid inclusions can lead to premature mechanical failure [61, 153, 154]. One paper highlighted that the addition of a 30% fill of ferroelectric powder to the elastomer decreased the strain limit from 500% to 200% [155].

LM droplets represent a promising alternative to rigid filler particles since they do not introduce significant stress concentrations or mechanical resistance. As with TEG and TENG devices, LMEE can again be used—in this case as a 'high-κ' dielectric material that generates power through its strain-based electromechanical coupling abilities [61]. This particular LMEE formulation uses EGaIn microdroplets on the order of ∼4–15 μm diameter. Compared to unfilled control samples, a 50% volume fraction filled LM composite increased the relative permittivity by 400%. A separate study has confirmed these permittivity results up to a 50% volumetric fill fraction [156]. The dissipation factor (D) of LMEE was found to be similar or less then unfilled elastomer ($D < 0.1$) [61]. Conversely a large dissipation factor for rigid high-κ composites materials can occur at fill fractions as low as 30 vol% [150]. Lastly, the electromechanical coupling of this material is excellent, with the ability to support up to 700% strain while having a relative capacitance increase of ∼4.5 at this extreme strain.

While LMEE composites with micron-sized inclusions have many excellent material attributes for DEGs, the material suffers from a low dielectric breakdown strength due to its heterogeneous microstructures. A previously fabricated microcomposite LMEE made with silicone elastomer (Ecoflex 30) has heterogeneous droplet sizes from as low as 4 μm to 15 μm with a breakdown field of 5.0 kV mm^{-1} [61]. A separate work on heterogeneous LMEE with average inclusion size of 47 μm and a matrix material of PDMS (Sylgard-184) produced a breakdown field of 2.1 kV mm^{-1} [85]. Comparatively, by controlling the droplet distributions to become homogenous with an average droplet size of ∼100 nm, recent work was able to sustain a breakdown

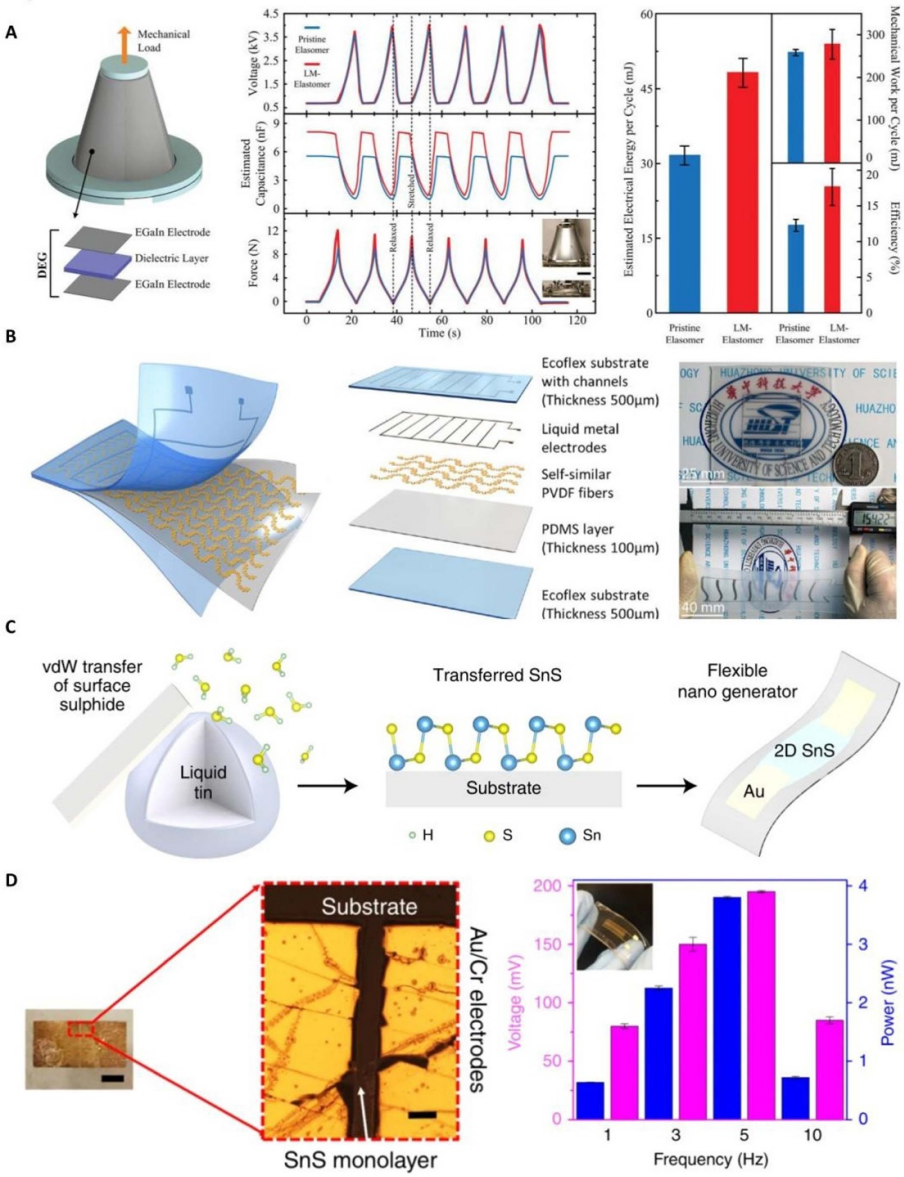

Figure 4. Liquid metals in electromechanical energy harvesters: (A) diagram of the first LMEE DEG with characterization vs virgin elastomer along with estimated electrical energy per cycle and efficiency comparisons between LMEE and virgin elastomer. Reproduced with permission [37], copyright 2019, WILEY-VCH Verlag GmbH & Co. KGaA. (B) Hyperstretchable TENG design using LM based architectures. Reproduced with permission [157], copyright 2017, Elsevier Ltd. (C) Monolayer SnS synthesis process for creating thin film piezoelectric generators. Reproduced with permission [158], copyright 2020, Springer Nature Limited. (D) Left: optical image of a two-electrode monolayer SnS piezoelectric generator. Scale bars are 1 mm and 50 μm. Right: power and voltage of piezoelectric generator as a function of tapping frequency. Reproduced with permission [158], copyright 2020, Springer Nature Limited.

field of 94.1 kV mm^{-1} [37]. In contrast, heterogeneous microcomposites have a lower breakdown strength due to large internal field concentrations that arise from the greater LM inclusion sizes. LMEE nanocomposites with homogenous inclusions of ~0.1–1 μm dimension were instead selected as the dielectric DEG since they enabled greater internal electric field and energy harvesting voltage output. Using the cone shaped design, the LMEE dielectric material was coated on both sides with a thin-film of EGaIn and cyclically displaced with an amplitude of 80 mm [37] (figure 4(a)). The LMEE-based DEG had a measured capacitance of 8.08 nF measured under 1 kHz at 1 V compared to 5.54 nF for the unfilled elastomer. This increased capacitance led to an estimated electrical energy that was 53% greater than unfilled elastomer. Compared to unfilled elastomers, the electrically efficiency of this device was increased from 12.3% to 17.7% with the incorporation of LM [37]. A separate study has confirmed 1 μm diameter droplets as the ideal droplet size for relative capacitance as a function of strain compared with 80 μm and 20 μm diameter droplets. This study used a 60 vol% fill fraction and recorded a relative capacitance increase of ~4× at 270% strain [56].

Recent advances in synthesis and integration of LM nanodroplets have significantly increased the number of promising matrix materials for DEG devices. For instance, surface-initiated atom transfer radical polymerization (SI-ATRP) has been recently introduced as a versatile synthesis method for LM-polymer nanocomposites with both thermoset and thermoplastic matrices [159, 160]. These advances have led to the most recent work on LM-based dielectric composites where EGaIn droplets with a poly (*n*-butyl methacrylate) coated shell are synthesized using ATRP [161]. At a 40 vol% LM, the relative permittivity was 22.5, much higher than previous work, and with a max strain above 400%. Compared to this latest work, the previous DEG work [37] recorded an ε_r of ∼11.5 at a 40 vol% LM for 10 μm dispersions and 8.8 at a 30 vol% for 1 μm dispersions. This study shows that future LM-DEG devices can show significantly higher performance if the composite parameters such as filler size, volume fraction, and polymer matrix are carefully selected.

5.2. Piezoelectric generators

5.2.1. Background on flexible piezoelectric materials

Conventional piezoelectric materials are solid ceramics such as lead zirconate titanate and lead magnesium niobite–lead titanate (PMN-PT), which have high electromechanical coupling coefficients [162–164]. However, these piezoelectric materials are stiff and mechanically incompatible for direct incorporation into wearable piezoelectric energy generators (PEGs) in its bulk form. Hence, these materials have been synthesized and integrated into polymer matrixes as microparticles or nanowires to combine the high compliance of the polymer with the high electromechanical coupling of the piezoelectric material. For instance, rigid piezoelectric PMN-PT microparticles, entangled with multiwalled carbon nanotubes, can be dispersed in soft silicone rubber as a compliant piezoelectric elastic composite (PEC) [165]. To ensure high performance of stretchable PEG, a highly compliant electrode also need to be accompanied. This is achieved by fabricating a pair of stretchable Ag very long nanowire percolation electrodes that cover the stretchable PEC substrate. The resultant PEG device exhibits a peak output voltage of 4 V and a stretchability up to 200% [165]. Despite Ag being stiff, its percolated networks of long (<500 μm) nanowires can be easily elongated with minimal resistance increments. These features ensure continuous accumulation of induced charges from variations of piezoelectric dipoles within PECs caused by stretching.

In addition to the high stiffness, the environmental concerns and toxicity of lead-based piezoelectric materials has also limited their applications for wearable devices. As a result, lead-free nano/micro materials such as $BaTiO_3$ [166, 167] and $0.5Ba(Zr_{0.2}Ti_{0.8})O_3–0.5(Ba_{0.7}Ca_{0.})TiO_{0.3}$ (BZT–BCT) [168, 169] have been reportedly synthesized and integrated into polymer matrixes as nanowires. Again, this material system serves to also combine the high mechanical compliance of polymers and the high electromechanical coupling of the nanowires, but now with biocompatibility concerns addressed for wearable application purposes.

Alternatively, researchers have also been using softer and biocompatible polymeric piezoelectric materials such as β-phase poly(vinylidene fluoride) (PVDF) [170–172] as the piezo component in PEGs (∼3 GPa). This allows for the fabrication of flexible PEGs in the form of woven or nonwoven micronsized fibers [173, 174] and PVDF coated hybrid-fiber nanogenerators [175] to enhance the flexibility of PEGs while having large electromechanical coupling. However, most of the flexible PEGs involving organic and inorganic piezoelectric materials, generate electrical power by bending or folding, but rarely from stretching, which is an important feature among wearables [176]. Hence, to fabricate flexible PEGs with better stretchability and piezoelectricity, stiff ceramic piezo materials (i.e. nano or macro) are incorporated into compliant polymers (i.e. elastomers) or piezoelectric polymers (PVDF) [166, 169, 175, 177, 178]. In these devices, composite conductors (elastomer and conductive microspheres) [177], sputtered metallic NPs (e.g. gold, aluminum and platinum) [166, 178], or in some cases thin layers (∼200 nm thick) of silver or gold, known as silver or gold leaf, have been used as electrode materials [169, 175]. These flexible PEGs have much smaller stretchable limits (<50%) than those of TEGs and TENGs (tables 1 and 2) that use LM composites or microfluidic interfaces.

5.2.2. LM for piezoelectric energy harvesters

This stretchability limitation among flexible piezoelectric energy harvesters can be rectified by using LM as microfluidic electrodes to enhance the stretchability, deformation detection limit, and fatigue life up to >300%, 280%, and >1400 cycles at a strain of 150% respectively [157]. In this work, an interdigitated LM microfluidic structure is employed to harness the accumulated charges from the polarized piezoelectric dipoles of self-similar serpentine structured micro/nanofibers of PVDF when stretched. This microfluidic channel is enclosed by a highly stretchable Ecoflex polymer in contact with the self-similar PVDF fibers. These fibers are also bonded on PDMS and another lower Ecoflex thin layer substrate (figure 4(b)). The use of soft polymer substrates and the combined serpentine and self-similar structure of PVDF nano/microfibers contributes to the functional stretchability of this stretchable PEG despite PVDF having much larger bulk

stiffness than PDMS and Ecoflex. With this capability, this PEG can function as a stretchable self-powered sensor which can stably detect its own deformation status and additional external stimuli such as amplitude and speed of external loading. Here, the LM microfluidics offer an alternative electrode with electrically and mechanically robust performance for the flexible piezoelectric devices in addition to other electrode material architectures reportedly used in this field such as woven/nonwoven conductive fibers or rigid conductive metal filler–rubber composites.

LM can also be used to synthesize novel piezoelectric materials other than functional materials such as electrodes or interconnects. Liquid tin and Ga can be the chemical substrate for self-limiting reactions to make homogenous, large area, and 2D atomically thin sheets of tin sulfide (SnS) monolayers and Ga phosphate respectively [158, 179]. For the synthesis of these SnS monolayers, the large surface tension found on the interface of liquid tin enables a growth of thin SnS (figure 4(c)). This synthesized 2D SnS has minimal grain boundaries, dislocations, and impurities when exposed to an anoxic environment containing sulfur compound for surface chemical reaction [158]. The flexible PEG developed with this material was able to generate a peak voltage of ∼190 mV and a maximum peak power output of 30.4 pW at a 5 Hz tapping frequency (figure 4(d)). In the case of Ga phosphate, a novel low temperature synthesis method of obtaining large lateral dimensions (i.e. in order of centimeters) of 2D Ga phosphate piezoelectric material is possible from harnessing the native Ga oxide thin film found on liquid Ga. This thin film is used as the substrate for chemical vapor reactions with phosphoric acid [179]. The resultant 2D Ga phosphate has large out of plane piezoelectricity (d_{33}) of 7.5 pm V^{-1} even at different thicknesses. This is deficient in many other existing successfully synthesized 2D piezoelectric materials (i.e. transitional-metal dichalcogenides), and an important feature for application in certain nanomechanical systems. In general, these 2D synthesized materials are flexible and have high piezoelectricity, both of which are ideal traits for fabricating flexible energy harvesters.

There are several techniques of enhancing the overall functional stretchability and flexibility of piezoelectric energy harvesting systems for better power performance. Some of these utilize piezoelectric nano or bulk materials with a high electromechanical coupling factor and structurally modifying their fabricated forms (i.e. fibers, textiles or composites). However, these desired features are often limited by the stretchability of the electrodes and the scalability or complexness of its processing. Hence, adapting LM based electrodes can potentially enhance the performance of these devices by introducing a more compliant, electrically robust, and scalable interface or electrode material.

6. Conclusions and outlook

LM material architectures such as LM microfluidics and LMEEs are unique materials in that they exhibit not only high thermal conductivity, electrical conductivity, and dielectric properties but also high stretchability, which is uncommon among metallic materials. As a result, this make them a suitable class of material for future advanced wearable energy harvesters. These material architectures can provide TEGs with stretchable and continuous thermal contact with the user's skin when deformed, ensuring that the thermal gradient within TEGs is maintained for maximum power output. Conductive LM pathways can act as deformable and stretchable interconnects for TEGs. Likewise, TENGs can utilize LM both as the dielectric component for electrostatic charge capture as well as for flexible and stretchable electrodes. Lastly, LM–polymer composites can be incorporated into DEGs as a stretchable high-κ dielectric material that can induce large capacitance changes when deformed, resulting in improved power output. Currently, LM material architectures have not been substantially utilized among PEGs because of its more limited potential for only supporting flexible and stretchable electrode functionality.

In the past few years, advances in synthesis of nanostructured LM material systems have significantly increased the number of emerging applications of LM including wearables and flexible energy harvesting. It is expected that new functional materials with a combination of LM fillers and active polymer matrices to be introduced for energy harvesting applications. There remain challenges in chemical stability of the active phases and their compatibility with Ga-based LM alloys. In addition, feasible and scalable integration and fabrication methods such as direct-writing and 3D printing should be developed to accelerate the transition of LM composites into emerging research fields as well as industries. From a biocompatibility perspective, further studies are required to rule out any potential health concern regarding the long-term use of Ga-based wearable energy harvesters with a direct contact with human skin. Lastly, computational and theoretical models should be developed to study the rate-dependent structural and functional behavior of LM material systems, which is essential for a variety of LM applications including soft and wearable energy harvesting devices.

We expect that in the future, these aforementioned wearable energy harvesting devices will be continually improved using previously mentioned LM approaches. This includes the incorporation of LM droplets in

elastomer to enhance the dielectric properties of DEGs and thermal properties of TEGs. Future efforts can also continue to explore the use of LM to improve stretchability of PENGs and TENGs and their conformability to the body. Further implementations should improve device performance and in-crease biocompatibility, ultimately bringing these devices closer to commercial use for IoT applications. Moreover, the mechanisms presented here are not the only types of energy harvesters that LMs will play a role in for future applications. Magneto-hydrodynamics [180] and reverse electrowetting (REWOD) generators [181] have incorporated LM into their devices for increased operation in the past. Magnetohydrodynamics uses LM as a conductive material that passes through a magnetic field, thus creating a potential difference. REWOD generators operate by harnessing the mechanical energy used to move conductive droplets across a potential difference. By forcing a change in charge configurations across these dielectric-coated electrodes, current is generated. Researchers have used these technologies in wearable applications, having demonstrated wrist worn magnetohydrodynamic generators [180] and shoe worn REWOD generators [181]. These applications highlight the future potential for these architectures as yet another area for LM to help advance research efforts in wearable energy harvesting in the future.

Acknowledgments

The authors acknowledge support from the AFOSR Multidisciplinary University Research Initiative (FA9550-18-1-0566; Program Manager: K Goretta) and the University of Washington Royalty Research Fund (Grant No. A153081).

ORCID iDs

Mason Zadan https://orcid.org/0000-0002-5718-3579
Carmel Majidi https://orcid.org/0000-0002-6469-9645
Mohammad H Malakooti https://orcid.org/0000-0002-7187-1706

References

[1] Wang J, Li S, Yi F, Zi Y, Lin J, Wang X, Xu Y and Wang Z L 2016 Sustainably powering wearable electronics solely by biomechanical energy *Nat. Commun.* **7** 1–8
[2] Gong S and Cheng W 2017 Toward soft skin-like wearable and implantable energy devices *Adv. Energy Mater.* **7** 1700648
[3] Nozariasbmarz A *et al* 2020 Review of wearable thermoelectric energy harvesting: from body temperature to electronic systems *Appl. Energy* **258** 114069
[4] Kim S J, Lee H E, Choi H, Kim Y, We J H, Shin J S, Lee K J and Cho B J 2016 High-performance flexible thermoelectric power generator using laser multiscanning lift-off process *ACS Nano* **10** 10851–7
[5] Mo X, Zhou H, Li W, Xu Z, Duan J, Huang L, Hu B and Zhou J 2019 Piezoelectrets for wearable energy harvesters and sensors *Nano Energy* **65** 104033
[6] Ghomian T and Mehraeen S 2019 Survey of energy scavenging for wearable and implantable devices *Energy* **178** 33–49
[7] Mitcheson P D, Yeatman E M, Rao G K, Holmes A S and Green T C 2008 Energy harvesting from human and machine motion for wireless electronic devices *Proc. IEEE* **96** 1457–86
[8] Jaziri N, Boughamoura A, Müller J, Mezghani B, Tounsi F and Ismail M 2019 A comprehensive review of thermoelectric generators: technologies and common applications *Energy Rep.* **6** 264–287
[9] Champier D 2017 Thermoelectric generators: a review of applications *Energy Convers. Manage.* **140** 167–81
[10] Riemer R and Shapiro A 2011 Biomechanical energy harvesting from human motion: theory, state of the art, design guidelines, and future directions *J. Neuroeng. Rehabil.* **8** 1–13
[11] Zou H *et al* 2019 Quantifying the triboelectric series *Nat. Commun.* **10** 1–9
[12] Zhou L, Liu D, Wang J and Wang Z L 2020 Triboelectric nanogenerators: fundamental physics and potential applications *Friction* **8** 481–506
[13] Kornbluh R D, Pelrine R, Prahlad H, Wong-Foy A, McCoy B, Kim S, Eckerle J and Low T 2012 Dielectric elastomers: stretching the capabilities of energy harvesting *MRS Bull.* **37** 246–53
[14] Carpi F, De Rossi D, Kornbluh R, Pelrine R E and Sommer-Larsen P 2011 *Dielectric Elastomers as Electromechanical Transducers: Fundamentals, Materials, Devices, Models and Applications of an Emerging Electroactive Polymer Technology* (Amsterdam: Elsevier)
[15] Koh S J A, Keplinger C, Li T, Bauer S and Suo Z 2011 Dielectric elastomer generators: how much energy can be converted? *IEEE/ASME Trans. Mechatronics* **16** 33–41
[16] Huang J, Shian S, Suo Z and Clarke D R 2013 Maximizing the energy density of dielectric elastomer generators using equi-biaxial loading *Adv. Funct. Mater.* **23** 5056–61
[17] Ramadan K S, Sameoto D and Evoy S 2014 A review of piezoelectric polymers as functional materials for electromechanical transducers *Smart Mater. Struct.* **23** 033001
[18] Na W S and Baek J 2018 A review of the piezoelectric electromechanical impedance based structural health monitoring technique for engineering structures *Sensors* **18** 1307
[19] Jung W S, Lee M J, Kang M G, Moon H G, Yoon S J, Baek S H and Kang C Y 2015 Powerful curved piezoelectric generator for wearable applications *Nano Energy* **13** 174–81
[20] Rupitsch S J 2018 *Piezoelectric Sensors and Actuators* (Berlin: Springer)
[21] Nakamura K 2012 *Ultrasonic Transducers: Materials and Design for Sensors, Actuators and Medical Applications* (Cambridge: Woodhead Publishing)

[22] Dagdeviren C *et al* 2014 Conformal piezoelectric energy harvesting and storage from motions of the heart, lung, and diaphragm *Proc. Natl Acad. Sci. USA* **111** 1927–1932
[23] Wang D, Yuan G, Hao G and Wang Y 2018 All-inorganic flexible piezoelectric energy harvester enabled by two-dimensional mica *Nano Energy* **43** 351–358
[24] Sun Y, Chen J, Li X, Lu Y, Zhang S and Cheng Z 2019 Flexible piezoelectric energy harvester/sensor with high voltage output over wide temperature range *Nano Energy* **61** 337–45
[25] Baek C, Yun J H, Wang J E, Jeong C K, Lee K J, Park K I and Kim D K 2016 A flexible energy harvester based on a lead-free and piezoelectric BCTZ nanoparticle-polymer composite *Nanoscale* **8** 17632–17638
[26] Cheng L, Yuan M, Gu L, Wang Z, Qin Y, Jing T and Wang Z L 2015 Wireless, power-free and implantable nanosystem for resistance-based biodetection *Nano Energy* **15** 598–606
[27] Zadan M, Malakooti M H and Majidi C 2020 Soft and stretchable thermoelectric generators enabled by liquid metal elastomer composites *ACS Appl. Mater. Interfaces* **12** 17921–8
[28] Nayak S, Li Y, Tay W, Zamburg E, Singh D, Lee C, Koh S J A, Chia P and Thean A V Y 2019 Liquid-metal-elastomer foam for moldable multi-functional triboelectric energy harvesting and force sensing *Nano Energy* **64** 103912
[29] Sargolzaeiaval Y, Padmanabhan Ramesh V, Neumann T V, Misra V, Vashaee D, Dickey M D and Öztürk M C 2020 Flexible thermoelectric generators for body heat harvesting—enhanced device performance using high thermal conductivity elastomer encapsulation on liquid metal interconnects *Appl. Energy* **262** 114370
[30] Pan C, Liu D, Ford M J and Majidi C 2020 Ultra-stretchable, wearable triboelectric nanogenerator based on sedimented liquid metal elastomer composite *Advanced Materials Technologies* **5** 2000754
[31] Bartlett M D, Kazem N, Powell-Palm M J, Huang X, Sun W, Malen J A and Majidi C 2017 High thermal conductivity in soft elastomers with elongated liquid metal inclusions *Proc. Natl Acad. Sci. USA* **114** 2143–8
[32] Park Y L, Chen B R and Wood R J 2012 Design and fabrication of soft artificial skin using embedded microchannels and liquid conductors *IEEE Sens. J.* **12** 2711–8
[33] Dickey M D 2014 Emerging applications of liquid metals featuring surface oxides *ACS Appl. Mater. Interfaces* **6** 18369–79
[34] Yang J, Cheng W and Kalantar-Zadeh K 2019 Electronic skins based on liquid metals *Proc. IEEE* **107** 2168–84
[35] Sun X, Wang X, Yuan B and Liu J 2020 Liquid metal–enabled cybernetic electronics *Mater. Today Phys.* **14** 100245
[36] Malakooti M H, Kazem N, Yan J, Pan C, Markvicka E J, Matyjaszewski K and Majidi C 2019 Liquid metal supercooling for low-temperature thermoelectric wearables *Adv. Funct. Mater.* **29** 1906098
[37] Pan C, Markvicka E J, Malakooti M H, Yan J, Hu L, Matyjaszewski K and Majidi C 2019 A liquid-metal–elastomer nanocomposite for stretchable dielectric materials *Adv. Mater.* **31** 1900663
[38] Plevachuk Y, Sklyarchuk V, Eckert S, Gerbeth G and Novakovic R 2014 Thermophysical properties of the liquid Ga-In-Sn eutectic alloy *J. Chem. Eng. Data* **59** 757–63
[39] Khoshmanesh K, Tang S Y, Zhu J Y, Schaefer S, Mitchell A, Kalantar-Zadeh K and Dickey M D 2017 Liquid metal enabled microfluidics *Lab Chip* **17** 974–93
[40] Wang X and Liu J 2016 Recent advancements in liquid metal flexible printed electronics: properties, technologies, and applications *Micromachines* **7** 206
[41] Zrnic D and Swatik D S 1969 On the resistivity and surface tension of the eutectic alloy of gallium and indium *J. Less-Common Met.* **18** 67–68
[42] Chiechi R C, Weiss E A, Dickey M D and Whitesides G M 2008 Eutectic gallium–indium (EGaIn): a moldable liquid metal for electrical characterization of self-assembled monolayers *Angew. Chem.* **47** 142–4
[43] Kim J H, Kim S, So J H, Kim K and Koo H J 2018 Cytotoxicity of gallium–indium liquid metal in an aqueous environment *ACS Appl. Mater. Interfaces* **10** 17448–54
[44] Zhu L, Wang B, Handschuh-Wang S and Zhou X 2020 Liquid metal–based soft microfluidics *Small* **16** 1903841
[45] Cheng S and Wu Z 2012 Microfluidic electronics *Lab Chip* **12** 2782–91
[46] Eaker C B and Dickey M D 2015 Liquid metals as ultra-stretchable, soft, and shape reconfigurable conductors *Micro- and Nanotechnology Sensors, Systems, and Applications VII* (https://doi.org/10.1117/12.2175988)
[47] Park Y L, Majidi C, Kramer R, Brard P and Wood R J 2010 Hyperelastic pressure sensing with a liquid-embedded elastomer *J. Micromech. Microeng.* **20** 6
[48] Boley J W, White E L, Chiu G T C and Kramer R K 2014 Direct writing of gallium-indium alloy for stretchable electronics *Adv. Funct. Mater.* **24** 3501–7
[49] Helseth L E 2018 Interdigitated electrodes based on liquid metal encapsulated in elastomer as capacitive sensors and triboelectric nanogenerators *Nano Energy* **49** 266–272
[50] Helseth L E 2019 Triboelectric proximity and contact detection using soft planar spiral electrodes *Smart Mater. Struct.* **28** 095009
[51] Wang S, Ding L, Fan X, Jiang W and Gong X 2018 A liquid metal-based triboelectric nanogenerator as stretchable electronics for safeguarding and self-powered mechanosensing *Nano Energy* **53** 863–70
[52] Yang Y *et al* 2018 Liquid-metal-based super-stretchable and structure-designable triboelectric nanogenerator for wearable electronics *ACS Nano* **12** 2027–34
[53] Dickey M D 2017 Stretchable and soft electronics using liquid metals *Adv. Mater.* **29** 1606425
[54] Dickey M D, Chiechi R C, Larsen R J, Weiss E A, Weitz D A and Whitesides G M 2008 Eutectic gallium-indium (EGaIn): a liquid metal alloy for the formation of stable structures in microchannels at room temperature *Adv. Funct. Mater.* **18** 1097–104
[55] Kazem N, Hellebrekers T and Majidi C 2017 Soft multifunctional composites and emulsions with liquid metals *Adv. Mater.* **29** 1605985
[56] Tutika R, Kmiec S, Tahidul Haque A B M, Martin S W and Bartlett M D 2019 Liquid metal-elastomer soft composites with independently controllable and highly tunable droplet size and volume loading *ACS Appl. Mater. Interfaces* **11** 17873–83
[57] Zhu L, Chen Y, Shang W, Handschuh-Wang S, Zhou X, Gan T, Wu Q, Liu Y and Zhou X 2019 Anisotropic liquid metal-elastomer composites *J. Mater. Chem.* C **7** 10166–72
[58] Wang H *et al* 2019 A highly stretchable liquid metal polymer as reversible transitional insulator and conductor *Adv. Mater.* **31** 1901337
[59] Xin Y, Peng H, Xu J and Zhang J 2019 Ultrauniform embedded liquid metal in sulfur polymers for recyclable, conductive, and self-healable materials *Adv. Funct. Mater.* **29** 1808989
[60] Yu Z *et al* 2018 A composite elastic conductor with high dynamic stability based on 3D-calabash bunch conductive network structure for wearable devices *Adv. Electron. Mater.* **4** 1800137

[61] Bartlett M D, Fassler A, Kazem N, Markvicka E J, Mandal P and Majidi C 2016 Stretchable, high-*k* dielectric elastomers through liquid-metal inclusions *Adv. Mater.* **28** 3726–31
[62] Fassler A and Majidi C 2015 Liquid-phase metal inclusions for a conductive polymer composite *Adv. Mater.* **27** 1928–32
[63] Tabor J, Chatterjee K and Ghosh T K 2020 Smart textile-based personal thermal comfort systems: current status and potential solutions *Adv. Mater. Technol.* **5** 1901155
[64] Wu H, Huang Y A, Xu F, Duan Y and Yin Z 2016 Energy harvesters for wearable and stretchable electronics: from flexibility to stretchability *Advanced Materials* **28** 9881–9919
[65] Siddique A R M, Mahmud S and Van Heyst B 2017 A review of the state of the science on wearable thermoelectric power generators (TEGs) and their existing challenges *Renew. Sustain. Energy Rev.* **73** 730–44
[66] Li C, Jiang F, Liu C, Liu P and Xu J 2019 Present and future thermoelectric materials toward wearable energy harvesting *Appl. Mater. Today* **15** 543–57
[67] Hong S, Lee S and Kim D H 2019 Materials and design strategies of stretchable electrodes for electronic skin and its applications *Proc. IEEE* **107** 2185–97
[68] Zhang M, Yao S, Rao W and Liu J 2019 Transformable soft liquid metal micro/nanomaterials *Mater. Sci. Eng.* R **138** 1–35
[69] Zheng Y, He Z, Gao Y and Liu J 2013 Direct desktop printed-circuits-on-paper flexible electronics *Sci. Rep.* **3** 1–7
[70] Zhu S, So J H, Mays R, Desai S, Barnes W R, Pourdeyhimi B and Dickey M D 2013 Ultrastretchable fibers with metallic conductivity using a liquid metal alloy core *Adv. Funct. Mater.* **23** 2308–2314
[71] Zhang X D, Yang X H, Zhou Y X, Rao W, Gao J Y, Ding Y J, Shu Q Q and Liu J 2019 Experimental investigation of galinstan based minichannel cooling for high heat flux and large heat power thermal management *Energy Convers. Manage.* **185** 248–58
[72] Joshipura I D, Ayers H R, Majidi C and Dickey M D 2015 Methods to pattern liquid metals *J. Mater. Chem.* C **3** 3834–41
[73] Kramer R K, Majidi C and Wood R J 2013 Masked deposition of gallium-indium alloys for liquid-embedded elastomer conductors *Adv. Funct. Mater.* **23** 5292–6
[74] Jeong S H, Hjort K and Wu Z 2015 Tape transfer atomization patterning of liquid alloys for microfluidic stretchable wireless power transfer *Sci. Rep.* **5** 8419
[75] Jeong S H, Hagman A, Hjort K, Jobs M, Sundqvist J and Wu Z 2012 Liquid alloy printing of microfluidic stretchable electronics *Lab Chip* **12** 4657–64
[76] Wissman J, Lu T and Majidi C 2013 Soft-matter electronics with stencil lithography *Proc. IEEE Sensors* (IEEE Computer Society) (https://doi.org/10.1109/ICSENS.2013.6688217)
[77] Liu J, Yang S, Liu Z, Guo H, Liu Z, Xu Z, Liu C and Wang L 2019 Patterning sub-30 um liquid metal wires on PDMS substrates via stencil lithography and pre-stretching *J. Micromech. Microeng.* **29** 95001
[78] Boley J W, White E L and Kramer R K 2015 Mechanically sintered gallium-indium nanoparticles *Adv. Mater.* **27** 2355–60
[79] Mohammed M G and Kramer R 2017 All-printed flexible and stretchable electronics *Adv. Mater.* **29** 1604965
[80] Liu S, Yuen M C, White E L, Boley J W, Deng B, Cheng G J and Kramer-Bottiglio R 2018 Laser sintering of liquid metal nanoparticles for scalable manufacturing of soft and flexible electronics *ACS Appl. Mater. Interfaces* **10** 28232–41
[81] Malakooti M H, Bockstaller M R, Matyjaszewski K and Majidi C 2020 Liquid metal nanocomposites *Nanoscale Adv.* **2** 2668–77
[82] Chen S, Wang H Z, Zhao R Q, Rao W and Liu J 2020 Liquid metal composites *Matter* **2** 1446–80
[83] Ford M J, Ambulo C P, Kent T A, Markvicka E J, Pan C, Malen J, Ware T H and Majidi C 2019 A multifunctional shape-morphing elastomer with liquid metal inclusions *Proc. Natl Acad. Sci. USA* **116** 21438–44
[84] Kazem N, Bartlett M D and Majidi C 2018 Extreme toughening of soft materials with liquid metal *Adv. Mater.* **30** 1706594
[85] Markvicka E J, Bartlett M D, Huang X and Majidi C 2018 An autonomously electrically self-healing liquid metal-elastomer composite for robust soft-matter robotics and electronics *Nat. Mater.* **17** 618–24
[86] Chen S, Wang H Z, Sun X Y, Wang Q, Wang X J, Chen L B, Zhang L J, Guo R and Liu J 2019 Generalized way to make temperature tunable conductor–insulator transition liquid metal composites in a diverse range *Mater. Horiz.* **6** 1854–61
[87] Fan P, Sun Z, Wang Y, Chang H, Zhang P, Yao S, Lu C, Rao W and Liu J 2018 Nano liquid metal for the preparation of a thermally conductive and electrically insulating material with high stability *RSC Adv.* **8** 16232–42
[88] Kang H, Zhao C, Huang J, Ho D H, Megra Y T, Suk J W, Sun J, Wang Z L, Sun Q and Cho J H 2019 Fingerprint-inspired conducting hierarchical wrinkles for energy-harvesting E-skin *Adv. Funct. Mater.* **29** 1903580
[89] Lai Y C, Deng J, Niu S, Peng W, Wu C, Liu R, Wen Z and Wang Z L 2016 Electric eel-skin-inspired mechanically durable and super-stretchable nanogenerator for deformable power source and fully autonomous conformable electronic-skin applications *Adv. Mater.* **28** 10024–32
[90] Wang X, Zhang Y, Zhang X, Huo Z, Li X, Que M, Peng Z, Wang H and Pan C 2018 A highly stretchable transparent self-powered triboelectric tactile sensor with metallized nanofibers for wearable electronics *Adv. Mater.* **30** 1706738
[91] Kim Y, Zhu J, Yeom B, Di Prima M, Su X, Kim J G, Yoo S J, Uher C and Kotov N A 2013 Stretchable nanoparticle conductors with self-organized conductive pathways *Nature* **500** 59–63
[92] Fan Y J, Meng X S, Li H Y, Kuang S Y, Zhang L, Wu Y, Wang Z L and Zhu G 2017 Stretchable porous carbon nanotube-elastomer hybrid nanocomposite for harvesting mechanical energy *Adv. Mater.* **29** 1603115
[93] Li S, Wang J, Peng W, Lin L, Zi Y, Wang S, Zhang G and Wang Z L 2017 Sustainable energy source for wearable electronics based on multilayer elastomeric triboelectric nanogenerators *Adv. Energy Mater.* **7** 1602832
[94] Lim G H, Kwak S S, Kwon N, Kim T, Kim H, Kim S M, Kim S W and Lim B 2017 Fully stretchable and highly durable triboelectric nanogenerators based on gold-nanosheet electrodes for self-powered human-motion detection *Nano Energy* **42** 300–6
[95] Suarez F, Nozariasbmarz A, Vashaee D and Öztürk M C 2016 Designing thermoelectric generators for self-powered wearable electronics *Energy Environ. Sci.* **9** 2099–113
[96] Goldsmid H 2014 Bismuth telluride and its alloys as materials for thermoelectric generation *Materials* **7** 2577–92
[97] Jeong S H, Cruz F J, Chen S, Gravier L, Liu J, Wu Z, Hjort K, Zhang S-L and Zhang Z-B 2017 Stretchable thermoelectric generators metallized with liquid alloy *ACS Appl. Mater. Interfaces* **9** 15791–7
[98] Chen Y, Zhao Y and Liang Z 2015 Solution processed organic thermoelectrics: towards flexible thermoelectric modules *Energy Environ. Sci.* **8** 401–22
[99] Takimiya K, Shinamura S, Osaka I and Miyazaki E 2011 Thienoacene-based organic semiconductors *Adv. Mater.* **23** 4347–70
[100] Huang L, Lin S, Xu Z, Zhou H, Duan J, Hu B and Zhou J 2020 Fiber-based energy conversion devices for human-body energy harvesting *Adv. Mater.* **32** 1902034
[101] Kim S J, We J H and Cho B J 2014 A wearable thermoelectric generator fabricated on a glass fabric *Energy Environ. Sci.* **7** 1959–65
[102] Lee J A *et al* 2016 Woven-yarn thermoelectric textiles *Adv. Mater.* **28** 5038–44

[103] Wang L and Zhang K 2020 Textile-based thermoelectric generators and their applications *Energy Environ. Mater.* **3** 67–79
[104] Yadav A, Pipe K P and Shtein M 2008 Fiber-based flexible thermoelectric power generator *J. Power Sources* **175** 909–13
[105] Zhang L, Lin S, Hua T, Huang B, Liu S and Tao X 2018 Fiber-based thermoelectric generators: materials, device structures, fabrication, characterization, and applications *Adv. Energy Mater.* **8** 1700524
[106] Du Y, Liu X, Xu J and Shen S Z 2019 Flexible Bi-Te-based alloy nanosheet/PEDOT:PSS thermoelectric power generators *Mater. Chem. Front.* **3** 1328–34
[107] Zhao X, Han W, Zhao C, Wang S, Kong F, Ji X, Li Z and Shen X 2019 Fabrication of transparent paper-based flexible thermoelectric generator for wearable energy harvester using modified distributor printing technology *ACS Appl. Mater. Interfaces* **11** 10301–9
[108] Karthikeyan V, Surjadi J U, Wong J C K, Kannan V, Lam K H, Chen X, Lu Y and Roy V A L 2020 Wearable and flexible thin film thermoelectric module for multi-scale energy harvesting *J. Power Sources* **455** 227983
[109] We J H, Kim S J and Cho B J 2014 Hybrid composite of screen-printed inorganic thermoelectric film and organic conducting polymer for flexible thermoelectric power generator *Energy* **73** 506–12
[110] Kim C S, Yang H M, Lee J, Lee G S, Choi H, Kim Y J, Lim S H, Cho S H and Cho B J 2018 Self-powered wearable electrocardiography using a wearable thermoelectric power generator *ACS Energy Lett.* **3** 501–7
[111] Hong S, Gu Y, Seo J K, Wang J, Liu P, Shirley Meng Y, Xu S and Chen R 2019 Wearable thermoelectrics for personalized thermoregulation *Sci. Adv.* **5** eaaw0536
[112] Yuan J and Zhu R 2020 A fully self-powered wearable monitoring system with systematically optimized flexible thermoelectric generator *Appl. Energy* **271** 115250
[113] Wang Y, Shi Y, Mei D and Chen Z 2018 Wearable thermoelectric generator to harvest body heat for powering a miniaturized accelerometer *Appl. Energy* **215** 690–8
[114] Jo S E, Kim M K, Kim M S and Kim Y J 2012 Flexible thermoelectric generator for human body heat energy harvesting *Electron. Lett.* **48** 1015–7
[115] Oh J Y *et al* 2016 Chemically exfoliated transition metal dichalcogenide nanosheet-based wearable thermoelectric generators *Energy Environ. Sci.* **9** 1696–705
[116] Ou C, Sangle A L, Datta A, Jing Q, Busolo T, Chalklen T, Narayan V and Kar-Narayan S 2018 Fully printed organic–inorganic nanocomposites for flexible thermoelectric applications *ACS Appl. Mater. Interfaces* **10** 19580–7
[117] Kim J Y, Oh J Y and Lee T I 2019 Multi-dimensional nanocomposites for stretchable thermoelectric applications *Appl. Phys. Lett.* **114** 043902
[118] Wang Y, Zhu W, Deng Y, Fu B, Zhu P, Yu Y, Li J and Guo J 2020 Self-powered wearable pressure sensing system for continuous healthcare monitoring enabled by flexible thin-film thermoelectric generator *Nano Energy* **73** 104773
[119] Chen B, Kruse M, Xu B, Tutika R, Zheng W, Bartlett M D, Wu Y and Claussen J C 2019 Flexible thermoelectric generators with inkjet-printed bismuth telluride nanowires and liquid metal contacts *Nanoscale* **11** 5222–30
[120] Xu B *et al* 2017 Nanocomposites from solution-synthesized PbTe-BiSbTe Nanoheterostructure with Unity figure of merit at low-medium temperatures (500–600 K) *Adv. Mater.* **29** 1605140
[121] Suarez F, Parekh D P, Ladd C, Vashaee D, Dickey M D and Öztürk M C 2017 Flexible thermoelectric generator using bulk legs and liquid metal interconnects for wearable electronics *Appl. Energy* **202** 736–45
[122] Crane D T and Bell L E 2006 Progress towards maximizing the performance of a thermoelectric power generator *Int. Conf. on Thermoelectrics, ICT, Proc.* pp 11–16
[123] Park H, Lee D, Kim D, Cho H, Eom Y, Hwang J, Kim H, Kim J, Han S and Kim W 2018 High power output from body heat harvesting based on flexible thermoelectric system with low thermal contact resistance *J. Phys. D: Appl. Phys.* **51** 365501
[124] Lee D, Park H, Park G, Kim J, Kim H, Cho H, Han S and Kim W 2019 Liquid-metal-electrode-based compact, flexible, and high-power thermoelectric device *Energy* **188** 116019
[125] Schneider F, Fellner T, Wilde J and Wallrabe U 2008 Mechanical properties of silicones for MEMS *J. Micromech. Microeng.* **18** 65008
[126] Tan S H, Nguyen N T, Chua Y C and Kang T G 2010 Oxygen plasma treatment for reducing hydrophobicity of a sealed polydimethylsiloxane microchannel *Biomicrofluidics* **4** 032204
[127] Zhou J, Khodakov D A, Ellis A V and Voelcker N H 2012 Surface modification for PDMS-based microfluidic devices *Electrophoresis* **33** 89–104
[128] Wang Y, Yang Y and Wang Z L 2017 Triboelectric nanogenerators as flexible power sources *npj Flex. Electron.* **1** 10
[129] Van De Graaff R J, Compton K T and Van Atta L C 1933 The electrostatic production of high voltage for nuclear investigations *Phys. Rev.* **43** 149–157
[130] Fan F R, Tian Z Q and Lin Wang Z 2012 Flexible triboelectric generator *Nano Energy* **1** 328–34
[131] Zhu G, Pan C, Guo W, Chen C Y, Zhou Y, Yu R and Wang Z L 2012 Triboelectric-generator-driven pulse electrodeposition for micropatterning *Nano Lett.* **12** 4960–4965
[132] Zhu G, Chen J, Zhang T, Jing Q and Wang Z L 2014 Radial-arrayed rotary electrification for high performance triboelectric generator *Nat. Commun.* **5** 1–9
[133] Yi F *et al* 2016 A highly shape-adaptive, stretchable design based on conductive liquid for energy harvesting and self-powered biomechanical monitoring *Sci. Adv.* **2** e1501624
[134] Wang X, Yin Y, Yi F, Dai K, Niu S, Han Y, Zhang Y and You Z 2017 Bioinspired stretchable triboelectric nanogenerator as energy-harvesting skin for self-powered electronics *Nano Energy* **39** 429–36
[135] Parida K, Kumar V, Jiangxin W, Bhavanasi V, Bendi R and Lee P S 2017 Highly transparent, stretchable, and self-healing ionic-skin triboelectric nanogenerators for energy harvesting and touch applications *Adv. Mater.* **29** 1702181
[136] Pu X, Liu M, Chen X, Sun J, Du C, Zhang Y, Zhai J, Hu W and Wang Z L 2017 Ultrastretchable, transparent triboelectric nanogenerator as electronic skin for biomechanical energy harvesting and tactile sensing *Sci. Adv.* **3** e1700015
[137] Khan M R, Eaker C B, Bowden E F and Dickey M D 2014 Giant and switchable surface activity of liquid metal via surface oxidation *Proc. Natl Acad. Sci. USA* **111** 14047–51
[138] Wu W *et al* 2019 Wearable high-dielectric-constant polymers with core-shell liquid metal inclusions for biomechanical energy harvesting and a self-powered user interface *J. Mater. Chem.* A **7** 7109–17
[139] Yang Y, Han J, Huang J, Sun J, Wang Z L, Seo S and Sun Q 2020 Stretchable energy-harvesting tactile interactive interface with liquid-metal-nanoparticle-based electrodes *Adv. Funct. Mater.* **30** 1909652

[140] Parida K, Thangavel G, Cai G, Zhou X, Park S, Xiong J and Lee P S 2019 Extremely stretchable and self-healing conductor based on thermoplastic elastomer for all-three-dimensional printed triboelectric nanogenerator *Nat. Commun.* **10** 1–9
[141] Wu Y, Luo Y, Qu J, Daoud W A and Qi T 2019 Liquid single-electrode triboelectric nanogenerator based on graphene oxide dispersion for wearable electronics *Nano Energy* **64** 103948
[142] Niu S and Wang Z L 2014 Theoretical systems of triboelectric nanogenerators *Nano Energy* **14** 161–92
[143] Ye Q *et al* 2019 Effects of liquid metal particles on performance of triboelectric nanogenerator with electrospun polyacrylonitrile fiber films *Nano Energy* **61** 381–8
[144] Lu T, Ma C and Wang T 2020 Mechanics of dielectric elastomer structures: a review *Extreme Mech. Lett.* **38** 100752
[145] Pelrine R, Kornbluh R D, Eckerle J, Jeuck P, Oh S, Pei Q and Stanford S 2001 Dielectric elastomers: generator mode fundamentals and applications *Smart Structures and Materials 2001: Electroactive Polymer Actuators and Devices* vol 4329, ed Y Bar-Cohen (SPIE) p 148
[146] McKay T, O'Brien B, Calius E and Anderson I 2010 An integrated, self-priming dielectric elastomer generator *Appl. Phys. Lett.* **97** 062911
[147] Suo Z, Zhao X and Greene W H 2008 A nonlinear field theory of deformable dielectrics *J. Mech. Phys. Solids* **56** 467–86
[148] Jiang Y, Liu S, Zhong M, Zhang L, Ning N and Tian M 2020 Optimizing energy harvesting performance of cone dielectric elastomer generator based on VHB elastomer *Nano Energy* **71** 104606
[149] Hammock M L, Chortos A, Tee B C K, Tok J B H and Bao Z 2013 25th anniversary article: the evolution of electronic skin (e-skin): a brief history, design considerations, and recent progress *Adv. Mater.* **25** 5997–6038
[150] Dang Z M, Yuan J K, Zha J W, Zhou T, Li S T and Hu G H 2012 Fundamentals, processes and applications of high-permittivity polymer-matrix composites *Prog. Mater. Sci.* **57** 660–723
[151] Bokobza L and Belin C 2007 Effect of strain on the properties of a styrene–butadiene rubber filled with multiwall carbon nanotubes *J. Appl. Polym. Sci.* **105** 2054–61
[152] Hassanen Jaber T K 2019 Stretchable multifunctional dielectric nanocomposites based on polydimethylsiloxane mixed with metal nanoparticles *Mater. Res. Express* **7** 105356
[153] Cho J, Joshi M S and Sun C T 2006 Effect of inclusion size on mechanical properties of polymeric composites with micro and nano particles *Compos. Sci. Technol.* **66** 1941–52
[154] Fu S Y, Feng X Q, Lauke B and Mai Y W 2008 Effects of particle size, particle/matrix interface adhesion and particle loading on mechanical properties of particulate-polymer composites *Composites* B **39** 933–61
[155] Gallone G, Carpi F, De Rossi D, Levita G and Marchetti A 2007 Dielectric constant enhancement in a silicone elastomer filled with lead magnesium niobate–lead titanate *Mater. Sci. Eng.* C **27** 110–6
[156] Koh A, Sietins J, Slipher G and Mrozek R 2018 Deformable liquid metal polymer composites with tunable electronic and mechanical properties *J. Mater. Res.* **33** 2443–53
[157] Huang Y, Ding Y, Bian J, Su Y, Zhou J, Duan Y and Yin Z 2017 Hyper-stretchable self-powered sensors based on electrohydrodynamically printed, self-similar piezoelectric nano/microfibers *Nano Energy* **40** 432–9
[158] Khan H *et al* 2020 Liquid metal-based synthesis of high performance monolayer SnS piezoelectric nanogenerators *Nat. Commun.* **11** 3449
[159] Yan J, Malakooti M H, Lu Z, Wang Z, Kazem N, Pan C, Bockstaller M R, Majidi C and Matyjaszewski K 2019 Solution processable liquid metal nanodroplets by surface-initiated atom transfer radical polymerization *Nat. Nanotechnol.* **14** 684–90
[160] Wei Q, Sun M, Wang Z, Yan J, Yuan R, Liu T, Majidi C and Matyjaszewski K 2020 Surface engineering of liquid metal nanodroplets by attachable diblock copolymers *ACS Nano* **14** 9884–9893
[161] Su Y, Sui G, Lan J and Yang X 2020 A highly stretchable dielectric elastomer based on core-shell structured soft polymer-coated liquid-metal nanofillers *Chem. Commun.* **56** 11625–11628
[162] Park K I *et al* 2014 Highly-efficient, flexible piezoelectric PZT thin film nanogenerator on plastic substrates *Adv. Mater.* **26** 2514–2520
[163] Xu S, Yeh Y W, Poirier G, McAlpine M C, Register R A and Yao N 2013 Flexible piezoelectric PMN-PT nanowire-based nanocomposite and device *Nano Lett.* **13** 2393–2398
[164] Qi Y, Jafferis N T, Lyons K, Lee C M, Ahmad H and McAlpine M C 2010 Piezoelectric ribbons printed onto rubber for flexible energy conversion *Nano Lett.* **10** 524–528
[165] Jeong C K *et al* 2015 A hyper-stretchable elastic-composite energy harvester *Adv. Mater.* **27** 2866–2875
[166] Malakooti M H, Julé F and Sodano H A 2018 Printed nanocomposite energy harvesters with controlled alignment of barium titanate nanowires *ACS Appl. Mater. Interfaces* **10** 38359–67
[167] Dudem B, Kim D H, Bharat L K and Yu J S 2018 Highly-flexible piezoelectric nanogenerators with silver nanowires and barium titanate embedded composite films for mechanical energy harvesting *Appl. Energy* **230** 865–874
[168] Wu W, Cheng L, Bai S, Dou W, Xu Q, Wei Z and Qin Y 2013 Electrospinning lead-free $0.5Ba(Zr_{0.2}Ti_{0.8})O_3$–$0.5(Ba_{0.7}Ca_{0.3})TiO_3$ nanowires and their application in energy harvesting *J. Mater. Chem.* A **1** 7332–8
[169] Zhou Z, Bowland C C, Malakooti M H, Tang H and Sodano H A 2016 Lead-free $0.5Ba(Zr_{0.2}Ti_{0.8})O_3$–$0.5(Ba_{0.7}Ca_{0.3})TiO_3$ nanowires for energy harvesting *Nanoscale* **8** 5098–105
[170] Yousry Y M, Yao K, Chen S, Liew W H and Ramakrishna S 2018 Mechanisms for enhancing polarization orientation and piezoelectric parameters of PVDF nanofibers *Adv. Electron. Mater.* **4** 1700562
[171] Lin J, Malakooti M H and Sodano H A 2020 Thermally stable poly(vinylidene fluoride) for high-performance printable piezoelectric devices *ACS Appl. Mater. Interfaces* **12** 21871–82
[172] Sappati K K and Bhadra S 2018 Piezoelectric polymer and paper substrates: a review *Sensors* **18** 3605
[173] Soin N *et al* 2014 Novel '3-D spacer' all fibre piezoelectric textiles for energy harvesting applications *Energy Environ. Sci.* **7** 1670–9
[174] Zeng W, Tao X-M, Chen S, Shang S, Chan H L W and Choy S H 2013 Highly durable all-fiber nanogenerator for mechanical energy harvesting *Energy Environ. Sci.* **6** 2631
[175] Lee M, Chen C-Y, Wang S, Cha S N, Park Y J, Kim J M, Chou L-J and Wang Z L 2012 A hybrid piezoelectric structure for wearable nanogenerators *Adv. Mater.* **24** 1759–64
[176] Fan F R, Tang W and Wang Z L 2016 Flexible nanogenerators for energy harvesting and self-powered electronics *Adv. Mater.* **28** 4283–305
[177] Niu X *et al* 2019 High-performance PZT-based stretchable piezoelectric nanogenerator *ACS Sustain. Chem. Eng.* **7** 979–85
[178] Dahiya A S, Morini F, Boubenia S, Nadaud K, Alquier D and Poulin-Vittrant G 2018 Organic/inorganic hybrid stretchable piezoelectric nanogenerators for self-powered wearable electronics *Adv. Mater. Technol.* **3** 1700249

[179] Syed N et al 2018 Printing two-dimensional gallium phosphate out of liquid metal Nat. Commun. 9 3618
[180] Jia D, Liu J and Zhou Y 2009 Harvesting human kinematical energy based on liquid metal magnetohydrodynamics Phys. Lett. A 373 1305–9
[181] Krupenkin T and Taylor J A 2011 Reverse electrowetting as a new approach to high-power energy harvesting Nat. Commun. 2 1–8